

# Transition signatures for electron-positron pair creation in space-time inhomogeneous electric field

C. K. Li,<sup>1</sup> X. X. Zhou,<sup>2</sup> Q. Chen,<sup>3</sup> B. An,<sup>4</sup> Y. J. Li,<sup>4,5</sup> N. S. Lin,<sup>5,\*</sup> and Y. Wan<sup>1,†</sup>

<sup>1</sup>Laboratory of Zhongyuan Light, School of Physics, Zhengzhou University, Zhengzhou 450001, China

<sup>2</sup>School of Management Science and Engineering, Anhui University of Finance and Economics, Bengbu 233030, China

<sup>3</sup>National Supercomputing Center in Zhengzhou, Zhengzhou University, Zhengzhou 450001, China

<sup>4</sup>State Key Laboratory for Tunnel Engineering, China University of Mining and Technology, Beijing 100083, China

<sup>5</sup>School of Science, China University of Mining and Technology, Beijing 100083, China

(Dated: August 20, 2024)

The process of electron-positron pair creation through multi-photon absorption in a space-time dependent electric field is analyzed using computational quantum field theory. Our findings reveal two distinct pair creation channels: the symmetric and asymmetric transition channels. We propose that the asymmetric transition channel arises from the inherent spatial inhomogeneity of intense laser pulses. By mapping the field-theoretical model of laser-assisted multi-photon pair creation onto a quantum-mechanical time-dependent framework, a semi-analytical solution that captures the asymmetric transition signatures of vacuum decay is derived. Additionally, it is demonstrated that neglecting spatial inhomogeneity leads to erroneous transition amplitudes and incorrect identification of pair creation channels, even when the dipole approximation holds.

The possibility of creating electron-positron pairs from the quantum vacuum state through the interaction with a supercritical external field is one of the most striking predictions of quantum electrodynamics[1–3]. There are two intrinsically different mechanisms by which electron-positron pairs can be created from the vacuum. The first scheme requires the field to be extremely strong and can be visualized as a tunneling process between energy-shifted Dirac states, known as the Schwinger mechanism[4]. The second scheme requires a very large laser frequency to trigger transitions between positive- and negative-energy states, referred to as the multi-photon mechanism[5]. Schwinger pair creation has not been directly verified in experiments due to the current highest laser intensity[6], approximately  $10^{23}$  W/cm<sup>2</sup>, is still significantly lower than the critical laser intensity of about  $10^{29}$  W/cm<sup>2</sup>. If the energy of multiple laser photons,  $n\omega$ , exceeds the gap between positive- and negative-energy continua,  $2m_e c^2 = 1.022$  MeV, then multi-photon pair creation can occur. The perturbative multi-photon pair production was observed at the Stanford Linear Accelerator Center (SLAC) E144 using nonlinear Compton scattering[7]. However, in this laser-electron collision, the findings were not conclusive, as the electron-positron pairs could be produced through either the Bethe-Heitler pair creation process or the multi-photon Breit-Wheeler process. Following this pioneering experiment, several laboratories around the world, including the Extreme Light Infrastructure[8], the Center for Relativistic Laser Science[9], the SLAC[10], the Rutherford Appleton Laboratory[11], the European X-Ray Free-Electron Laser[12] and Shanghai Superintense Ultrafast Laser Facility[13], are actively developing new methods to probe the quantum vacuum properties using very intense electromagnetic fields.

In addition to experimental efforts, researchers have explored electron-positron pair creation using theoretical methods. The multi-photon pair creation process has been extensively studied by modeling the laser as a spatially homogeneous alternating electric field[14–17]. However, realistic

ultra-strong fields, generated by short-pulse, focused lasers, introduce significant spatial inhomogeneity, which plays a critical role in pair creation. Several studies have examined the intriguing phenomena of pair creation induced by spatiotemporally inhomogeneous fields[18–26]. One of the key observations is the occurrence of asymmetric multi-photon transitions, which differ from the more commonly observed symmetric transitions. In intuitive terms, symmetric transition involves an electron moving from an initial negative-energy state  $E_n = -\hbar\omega/2$  to a final positive-energy state  $E_p = \hbar\omega/2$  (see the red dashed line in Fig. 1). Asymmetric transition, on the other hand, involves an electron transitioning from  $E_n \neq -\hbar\omega/2$  to  $E_p \neq \hbar\omega/2$  with the satisfaction of energy conservation  $E_p - E_n = \hbar\omega$  (see the blue solid lines in Fig. 1). Recently, asymmetric transitions were observed in an idealized external field composed of a temporally periodic vector field  $A(t) = A_0 \cos(\omega t)$  and a spatially periodic scalar field  $V(z) = V_0 \cos(kz)$ [26]. However, such a field structure is highly specialized and challenging to realize with practical laser pulses. In this Letter, we present a generalized model demonstrating that the asymmetric transition channel is directly related to the spatial width of a single external field.

For this purpose, we utilize a spatiotemporally inhomogeneous electric field with a peak field strength  $A_0$ , space width  $\lambda$  and oscillation frequency  $\omega$  of the form

$$A(z, t) = A_0 \exp(-z^2/2\lambda^2) \cos(\omega t) f(t). \quad (1)$$

The field can be conceptualized as a model of the electric field in a standing-wave mode formed by two counter-propagating laser pulses. We focus solely on the envelope of the standing wave and neglect the effects of photon momentum  $k$ , thereby removing the term  $\sin(kz)$  from the standing wave field. The time-dependent function  $f(t)$  in Eq. 1 is employed to simulate the turn-on and turn-off processes. Its turn-on for  $0 \leq t \leq T_L$  is given as  $f(t) = \sin^2[\pi t/(2T_L)]$ , which is then followed by a constant plateau region  $T_L \leq t \leq 19T_L$  with  $f(t) = 1$ . Finally, for  $19T_L \leq t \leq 20T_L$ , the field is turned off, described

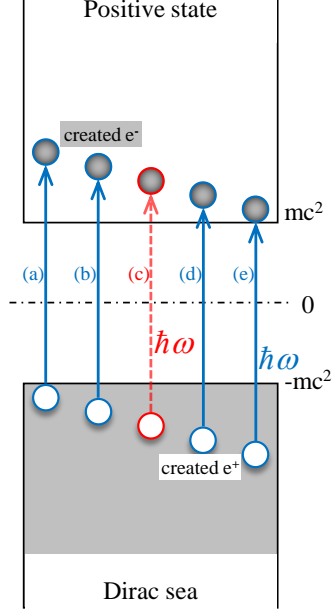


FIG. 1. The scheme of multi-photon electron-positron pair creation. The asymmetrical transition are represented by (a), (b), (d), and (e), while the symmetrical transition is shown in (c).

by  $f(t) = \cos^2[(\pi t - 19T_L)/(2T_L)]$ . Here,  $T_L = 2\pi/\omega$  represents the optical period of the laser pulse and denotes the duration for turn-on and turn-off processes. In our study, we introduce the transition probability for electrons in the negative states and find noticeable asymmetric transition signatures. These signatures are explained by relating the quantum field approach to the quantum mechanical perturbation description. Moreover, we observe the slightly unrealistic nature of the assumption of spatial homogeneity.

Let us first briefly summarize our approach based on computational quantum field theory[27–29]. The interaction of the electromagnetic field with the electron-positron quantum field operator is described by the usual Dirac Hamiltonian

$$H = c\sigma_1[p_z - qA(z, t)/c] + mc^2\sigma_3, \quad (2)$$

where  $\sigma_1$  and  $\sigma_3$  are the  $2 \times 2$  Pauli matrices,  $m$  and  $q$  are the electron's mass and charge, and  $c$  is the speed of light. The characteristic spatial and temporal scales for the dynamics are naturally provided by the electrons' Compton wavelength  $\lambda_c \equiv \hbar/(mc) = 3.9 \times 10^{-13}m$  and the corresponding time  $T \equiv \hbar/(mc^2) = 1.3 \times 10^{-21}s$ . The field operator can be expanded as

$$\begin{aligned} \hat{\psi}(z, t) &= \sum_p \hat{b}_p(t)u_p(z) + \sum_n \hat{d}_n^\dagger(t)v_n(z) \\ &= \sum_p \hat{b}_p u_p(z, t) + \sum_n \hat{d}_n^\dagger v_n(z, t). \end{aligned} \quad (3)$$

Here,  $\hat{b}_p(t)$ ,  $\hat{d}_n^\dagger(t)$ ,  $\hat{b}_p$  and  $\hat{d}_n^\dagger$  are the particle annihilation and the anti-particle creation operators, respectively. The field-free Hamiltonian  $H_0 = c\sigma_1 p_z + m\sigma_3 c^2$  at  $t = 0$ , and its energy eigenstates are  $u_p(z)$  ( $E \geq mc^2$ ) and  $v_n(z)$  ( $E \leq -mc^2$ ).  $u_p(z, t)$  and  $v_n(z, t)$  are respectively the time evolved states of  $u_p(z)$  and  $v_n(z)$ , and their evolution satisfy the Dirac equation  $i\hbar\partial_t\hat{\Psi}(z, t) = H\hat{\Psi}(z, t)$ . The time evolution of the fermion annihilation and creation operators are

$$\begin{aligned} \hat{b}_p(t) &= \sum_{p'} \hat{b}_{p'} \langle p|U(t)|p'\rangle + \sum_{n'} \hat{d}_{n'}^\dagger \langle p|U(t)|n'\rangle, \\ \hat{d}_n^\dagger(t) &= \sum_{p'} \hat{b}_{p'} \langle n|U(t)|p'\rangle + \sum_{n'} \hat{d}_{n'}^\dagger \langle n|U(t)|n'\rangle. \end{aligned} \quad (4)$$

Here, the anti-commutation relations  $[\hat{b}_p, \hat{b}_{p'}^\dagger]_+ = \delta_{p,p'}$ ,  $[\hat{d}_n, \hat{d}_{n'}^\dagger]_+ = \delta_{n,n'}$  are applied.  $U(t)$  represents the time evolution operator that governs the evolution of the quantum state over time according to the Dirac equation,  $|p\rangle = u_p(z)$  and  $|n\rangle = v_n(z)$ . The time dependence of the total number of created electron-positron pairs is defined by the vacuum expectation value of products of the creation and annihilation operators

$$N_{tot}(t) = \sum_{p,n} \langle \langle \text{vac} | \hat{b}_p^\dagger(t) \hat{b}_p(t) | \text{vac} \rangle \rangle = \sum_{p,n} |U_{p,n}(t)|^2. \quad (5)$$

These solutions of the space-time dependent Dirac equation with the vector potential  $A(z, t)$  can be obtained on a space-time lattice using efficient fast-Fourier transformation based split-operator techniques.

In computational quantum field theory, an intuitive graphical interpretation of the electron-positron pair creation process is possible. The transition amplitude is determined by projecting the negative energy states  $|E_n(t)\rangle$  onto the initial positive energy states  $|E_p\rangle$  at time  $t$ . In this scenario, all external fields are simultaneously turned off at a specific time  $t$ , and the resulting time-dependent number of created particles represents the actual physical count of particles[30]. In our method,  $|U_{p,n}(t)|^2$  represents the expectation value of the number of created pairs with momentum  $p$  and  $n$ . The energy of the positive state is given by  $E_p = \sqrt{p^2 c^2 + c^4}$ , while the energy of the negative state is  $E_n = -\sqrt{n^2 c^2 + c^4}$ . Therefore,  $|\langle E_p | E_n(t) \rangle|^2 = |U_{E_p, E_n}(t)|^2$  can be interpreted as the probability of an electron transitioning from a negative energy state  $|E_n\rangle$  to a positive energy state  $|E_p\rangle$  at time  $t$ .

The most remarkable effect is that the electron-positron pair creation process exhibits asymmetric transition signatures, with an asymmetric transition scale determined by the spatial extent of the laser pulse, as shown in Fig. 2. The horizontal axis represents negative energy, while the vertical axis represents positive energy. The transition probabilities for specific states are indicated by the color scale. The “anti-diagonal line” in the southwest-to-northeast facing diagonal denotes symmetric transitions with opposite momentum (identical absolute value) and symmetric energy. Conversely,

the area outside this line denotes asymmetric transitions with different momentum and asymmetric energy. Due to the energy conservation  $E_p - E_n - \hbar\omega = 0$ , the transition probability of the electron exhibits a "block" shape. Note that the multi-photon pair creation proceeds via both resonance and non-resonance transition paths[18, 31].

In order to get a better idea how this asymmetric transition is possible, we performed simulations for two critical case. In Fig. 2 (a), we illustrate the transition probability of the electron when the spatial width  $\lambda$  is equal to the electrons' Compton wavelength  $\lambda_c$ . The electrons' Compton wavelength  $\lambda_c$  is the minimum spatial length for electron-positron pair creation. In this case, electron-positron pairs are created by both the symmetric transition channel and the asymmetric transition channel, with the asymmetric transition channel accounting for the vast majority of the total yield. For the case of maximal spatial width,  $\lambda$  is infinite, as shown in Fig. 2 (b). The dipole approximation is expected to be well justified in optical laser fields, where the laser spatial width  $\lambda$  is much larger than the Compton wavelength  $\lambda_c$ :  $\lambda \gg \lambda_c$ [32]. Therefore, the external electric field is equivalent to a spatially uniform and time-dependent field  $A(t) = A_0 \cos(\omega t) f(t)$  when the spatial width  $\lambda$  is infinite. In our simulation, we use the electric field  $A(t) = A_0 \cos(\omega t) f(t)$  instead of the field  $A(z, t) = A_0 \exp(-z^2/2\lambda^2) \cos(\omega t) f(t)$  for the case of infinite spatial width. In contrast to the space-dependent electric field  $A(z, t)$ , where the asymmetric transition channel vanishes and the symmetric transition channel is enhanced. It is suggested that the spatial inhomogeneity of the field can trigger numerous irreversible transitions from each negative energy state to each positive energy state, thereby opening the asymmetric transition channel. On the other hand, the spatially uniform electric field  $A(t) = A_0 \cos(\omega t) f(t)$ , where the dipole approximation was well justified, incorrectly predicts the creation of electron-positron pairs. Due to the assumption of spatial homogeneity, it does not account for the asymmetric transitions that would occur. In addition, the symmetric transition probability for this case is approximately four orders of magnitude greater than that when the spatial width  $\lambda$  equals the Compton wavelength  $\lambda_c$ . This is because the field strength throughout the entire numerical box is maximal when the spatial width is infinite.

We have computed the pair-creation number  $N_{sym}(t)$  and  $N_{asy}(t)$  to examine the asymmetric transition process more quantitatively. The term  $N_{sym}(t)$  denotes the pair-creation number from the symmetric transition process, defined as  $N_{sym}(t) = \sum_{p,n} |U_{p,n}(t)|^2$ ,  $|p| = |n|$ . The number  $N_{asy}(t)$  is defined as  $N_{asy}(t) = \sum_{p,n} |U_{p,n}(t)|^2$ ,  $|p| \neq |n|$ , representing the electron-positron pairs created by the asymmetric transition path. In Fig. 3, we depict the spatial dependence of the pair-creation numbers  $N_{sym}(t = 20T_L)$  and  $N_{asy}(t = 20T_L)$ . We see that, for the same values of the other parameters, the pair-creation number increases with the spatial width of the field. Furthermore, we have observed that increasing the spatial width  $\lambda$  leads to a significant reduction

in the slope of the function  $N_{asy}(\lambda, 20T_L)$ . Conversely, increasing  $\lambda$  enhances the slope of the function  $N_{sym}(\lambda, 20T_L)$ . Based on Fig.2 and Fig.3, we predict that the pair-creation number  $N_{sym}(\lambda, 20T_L)$  equals  $N_{asy}(\lambda, 20T_L)$  at a certain spatial width  $\lambda$ . Beyond this spatial width,  $N_{sym}(\lambda, 20T_L)$  is anticipated to exceed  $N_{asy}(\lambda, 20T_L)$  in magnitude.

To understand the physical origin of the asymmetric transition channel, we recall that, for a space-time dependent electric field, the pair creation process can be viewed as a time-dependent perturbation problem. The Fig. 3 also displays the time-dependent pair-creation number predicted by perturbation theory. While the pair creation numbers  $N'_{asy}(\lambda, 20T_L)$  for the asymmetric transition process show slow growth with increasing spatial width  $\lambda$ ,  $N'_{sym}(\lambda, 20T_L)$  exhibits rapid growth. However, the error of the computational quantum field theory and the first-order perturbation theory increases as the spatial width  $\lambda$  increases. This is due to the fact that the field strength increases across the entire numerical box as  $\lambda$  increases.

We consider first-order time-dependent perturbation theory to theoretically describe the single-photon transition. Since the interaction does not couple spin directions, we can express the field operator using only two components. The Hamiltonian of this system can then be separated into two parts:  $H = H_0 + H'$ , where the external field is represented by  $H' = -q\sigma_1 A(z, t)$ , treated as a perturbation, and  $H_0$  is the field-free Hamiltonian, analogous to the computational quantum field theory. The first-order transition amplitude from the negative state  $|n\rangle$  to the positive state  $|p\rangle$  at an arbitrary time  $t$  is given by

$$C_{p,n}(t) = \int_0^t \langle p | H' | n \rangle \exp[i(E_p - E_n)\tau] / i d\tau. \quad (6)$$

By summing over all the states of  $p$  and  $n$ , we derive the first-order perturbation estimate of the total pair creation as

$$N'_{tot}(t) = \sum_{p,n} |C_{p,n}(t)|^2 = \sum_{p,n} |\langle p | -q\sigma_1 A(z) | n \rangle| \times \{ \exp[i(E_p - E_n - \hbar\omega)t] - 1 \} / (E_p - E_n - \hbar\omega)^2 \quad (7)$$

The inner product  $\langle p | -q\sigma_1 A(z) | n \rangle$  is known as the coupling strength  $\kappa(\lambda)$  in quantum mechanics,

$$\kappa(\lambda) = 2\pi A_0^2 \lambda^2 A_{p,n} \exp[-(p+n)^2 \lambda^2 / 2]^2 \quad (8)$$

where the inner product for spins  $A_{p,n}$  is defined as  $[sgn(n)\sqrt{E_p + c^2}\sqrt{-E_n - c^2} + sgn(p)\sqrt{E_p - c^2}\sqrt{-E_n + c^2}] / [4\pi\sqrt{-E_p E_n}]$ . We found that the energy conservation term in the total creation number  $N'_{tot}(t)$  (see Eq. 7) is an exponential function  $\{ \exp[i(E_p - E_n - \hbar\omega)t] - 1 \} / (E_p - E_n - \hbar\omega)$ , rather than a delta function  $\delta(E_p - E_n - \hbar\omega)$ . Therefore, the transition probability of the electron displays a "block" shape that includes the non-resonant transition path. Similarly, the perturbative estimates of the number of symmetrically created pairs  $N'_{sym}(t)$  and asymmetrically created pairs

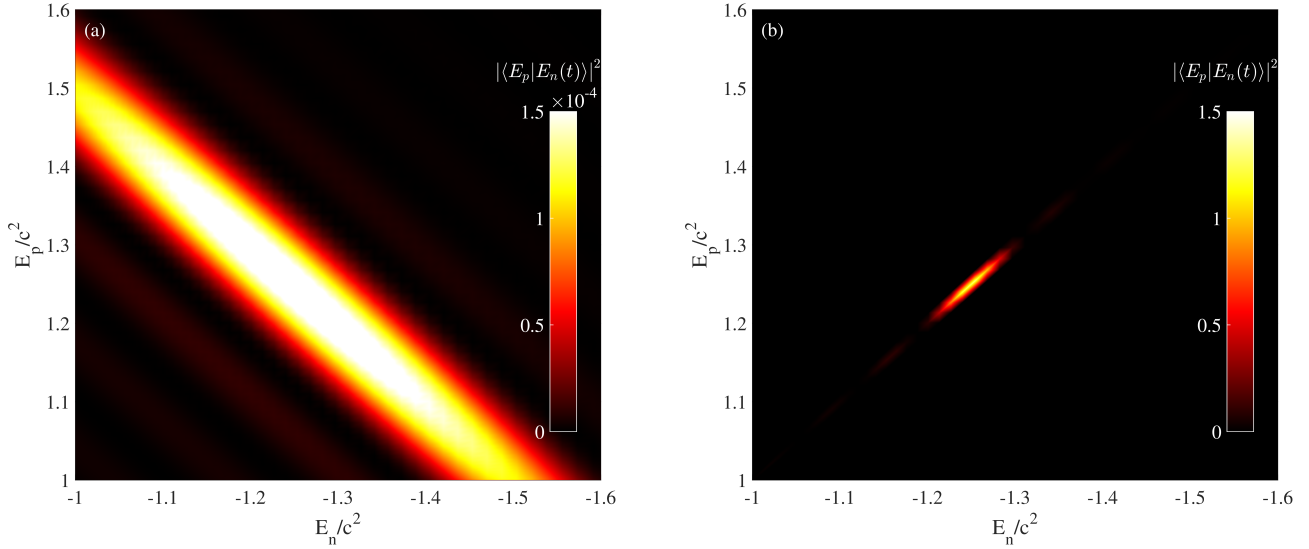


FIG. 2. The transition probability of electron for different space width (a)  $\lambda = \lambda_c$ , (b)  $\infty$ . The parameters are  $A_0 = 0.05mc^2$ ,  $\hbar\omega = 2.5mc^2$ ,  $t = 20T_L$ .

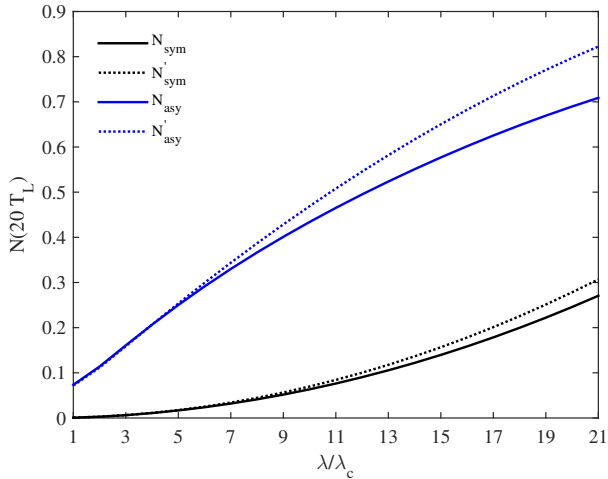


FIG. 3. The space dependence of the created pairs as a function of field space extent  $\lambda$  (in units of the electrons' Compton wavelength  $\lambda_c$ ). The solid line and the dashed line represent the results of computational quantum field theory and time-dependent perturbation theory, respectively. The parameters are  $A_0 = 0.05mc^2$ ,  $\hbar\omega = 2.5mc^2$ ,  $t = 20T_L$ .

$N'_{asy}(t)$  are obtained by summing over the corresponding states of  $p$  and  $n$ . The excellent match of  $N'_{sym}(\lambda, 20T_L)$  and  $N'_{asy}(\lambda, 20T_L)$  with the numerical data suggests that the first-order time-dependent perturbation theory can indeed capture the main features of the single-photon transition process.

This indicates that the asymmetric transition can be attributed to the spatial dependence of the coupling strengths  $\kappa(\lambda)$  (see Eq. 8). In Fig. 4, we have graphed the coupling

strengths  $\kappa(\lambda, E_n, E_p)$  between the negative energy  $E_n$  and the positive energy  $E_p$  for  $\lambda = \lambda_c$  and  $\lambda = \infty$ . We observe that the coupling strength  $\kappa(\lambda = \lambda_c, E_n, E_p)$  is universally applicable across the entire energy range, whereas the coupling strengths  $\kappa(\lambda = \infty, E_n, E_p)$  is valid only for symmetric negative and positive states. Comparing with Fig. 2, asymmetric transitions are permitted for the space-dependent field  $A(z, t)$ , whereas asymmetric transitions are not permitted for the space-independent field  $A(t)$ . It is immediately clear how asymmetric transition signatures arise in the more realistic case of additional spatial pulse inhomogeneities. From a mathematical point of view, this exponential term  $\exp[-(p+n)^2\lambda^2/2]^2$  in the coupling strengths  $\kappa(\lambda = \infty, E_n, E_p)$  equals "1" only when  $p+n=0$  and  $\exp[-(p+n)^2\lambda^2/2]^2 = 0$  for  $p+n \neq 0$ . This indicates conservation of the total canonical momentum of the system, which exclusively opens symmetric transition channels. For a finite spatial width of the field,  $\lambda \neq \infty$ , the exponential term  $\exp[-(p+n)^2\lambda^2/2]^2$  is non-zero for asymmetric negative and positive states. This suggests that under these conditions, asymmetric transitions between negative and positive states are possible. In other words, the asymmetric transition due to the spatial inhomogeneities of field  $A(z, t)$  (compared to  $A(t)$ ) becomes important. If the spatial dependence of the electric field is neglected, even though the dipole approximation is well justified, the asymmetric transitions will vanish. This leads to an unphysical prediction for the electron-positron pair creation process in the space-dependent field  $A(z, t)$ . The study suggests that the inevitable spatial inhomogeneity of electric fields significantly impacts the electron-positron pair creation process from the vacuum.

In summary, electron-positron pair creation in spatially and temporally inhomogeneous electric fields has been studied

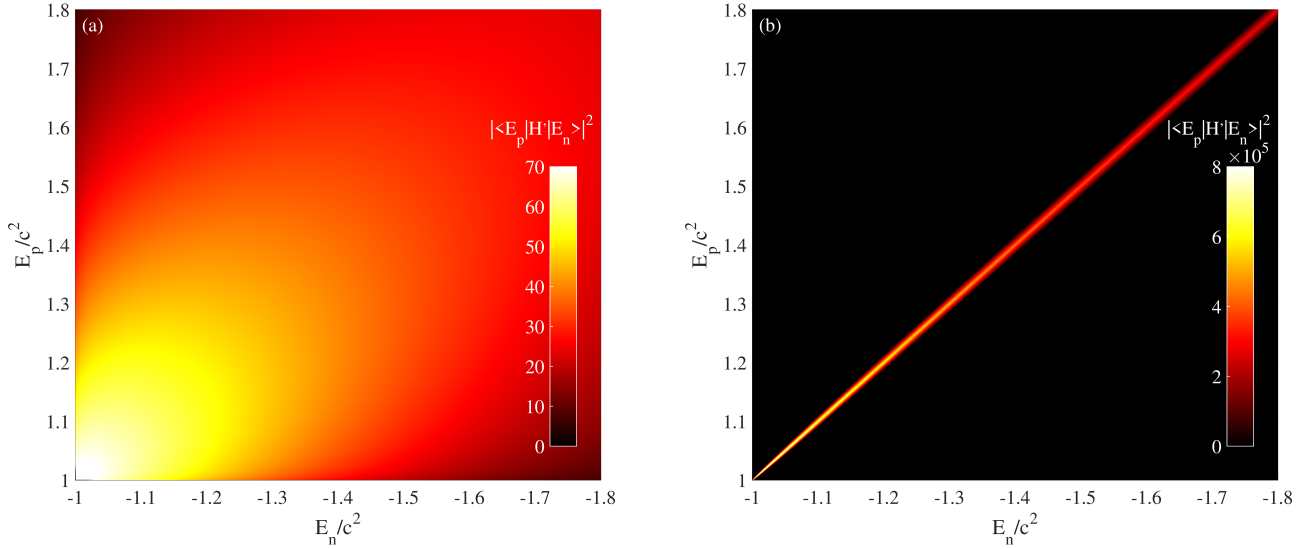


FIG. 4. The coupling strengths  $\kappa(\lambda, E_n, E_p)$  of initial energy state for different spatial width (a)  $\lambda = \lambda_c$ , (b)  $\lambda = \infty$ . The parameters are  $A_0 = 0.05mc^2$ .

both numerically and theoretically. We have demonstrated that the spatial extent of the field suppresses the asymmetric transition pathway while enhancing the symmetric transition pathway. From a theoretical viewpoint, we find that the spatial inhomogeneity of the field brings about the asymmetric multi-photon transition channels. When the laser wavelength is much larger than the electrons' Compton wavelength, the dipole approximation is satisfied in electron-positron pair creation. However, the omission of the laser's spatial inhomogeneity changes the entire pair-creation process and therefore leads to unreliable predictions. Consequently, the transition amplitude of the electron is qualitatively incorrect and excludes the physical asymmetric transition process.

This work has been supported by the National Natural Science Foundation of China (NSFC) under Grants No.12204001. Numerical simulations were implemented on the SongShan supercomputer at National Supercomputing Center in Zhengzhou.

\* phy.nslin@gmail.com

† yangwan23@zzu.edu.cn

- [1] A. Di Piazza, C. Müller, K. Z. Hatsagortsyan and C. H. Keitel, Extremely high-intensity laser interactions with fundamental quantum systems, *Rev. Mod. Phys.* **84**, 1177 (2012).
- [2] A. Fedotov, A. Ilderton, F. Karbstein *et al.*, Advances in QED with intense background fields, *Physics Reports* **1010**, 1 (2023).
- [3] T. P. Yu, K. Liu, J. Zhao *et al.*, Bright X/ $\gamma$ -ray emission and lepton pair production by strong laser fields: a review, *Rev. Mod. Plasma Phys.* **8**, 24 (2024).
- [4] J. Schwinger, On Gauge Invariance and Vacuum Polarization, *Phys. Rev.* **82**, 664 (1951).
- [5] E. Brezin and C. Itzykson, Pair Production in Vacuum by an

Alternating Field, *Phys. Rev. D* **2**, 1191 (1970).

- [6] W. Y. Jin, G. K. Yeong, W. C. II *et al.*, Realization of laser intensity over  $10^{23}$  W/cm<sup>2</sup>, *Optica* **8** 630-635 (2021).
- [7] D. L. Burke, R. C. Field, G. Horton-Smith *et al.*, Positron Production in Multiphoton Light-by-Light Scattering, *Phys. Rev. Lett.* **79**, 1626 (1997).
- [8] See <https://eli-laser.eu>; I. C. E. Turcu, F. Negoita, D. A. Jaroszynski *et al.*, High Field Physics and QED experiments at ELI-NP, *Rom. Rep. Phys.* **68**, S145 (2016).
- [9] See <https://corels.ibs.re.kr>.
- [10] S. Meuren, E-20 collaboration at FACET-II, <https://facet.slac.stanford.edu>.
- [11] C. H. Keitel, A. Di Piazza, G. G. Paulus *et al.*, Photo-induced pair production and strong field QED on Gemini, [arXiv:2103.06059](https://arxiv.org/abs/2103.06059), (2021).
- [12] See <http://www.hibef.eu>; H. Abramowicz, U. Acosta, M. Altarelli *et al.*, Conceptual design report for the LUXE experiment, *Eur. Phys. J.: Spec. Top.* **230**, 2445 (2021).
- [13] W. Q. Li, Z. B. Gan, L. H. Yu *et al.*, 339 J high-energy Ti: sapphire chirped-pulse amplifier for 10 PW laser facility, *Opt. Lett.* **43**, 5681-5684 (2018).
- [14] S. S. Bulanov, N. B. Narozhny, V. D. Mur and V. S. Popov, Electron-positron pair production by electromagnetic pulses, *J. Exp. Theor. Phys.* **102**, 9 (2006).
- [15] C. Kohlfürst, H. Gies and R. Alkofer, Effective Mass Signatures in Multiphoton Pair Production, *Phys. Rev. Lett.* **112**, 050402 (2014).
- [16] H. Taya, T. Fujimori, T. Misumi *et al.*, Exact WKB analysis of the vacuum pair production by time-dependent electric fields, *J. High Energ. Phys.* **2021**, 82 (2021).
- [17] R. Z. Jiang, C. Gong, Z. L. Li and Y. J. Li, Backreaction effect and plasma oscillation in pair production for rapidly oscillating electric fields, *Phys. Rev. D* **108**, 076015 (2023).
- [18] M. Ruf, G. R. Mocken, C. Müller *et al.*, Pair Production in Laser Fields Oscillating in Space and Time, *Phys. Rev. Lett.* **102**, 080402 (2009).
- [19] K. Krajewska and J. Z. Kamiński, Recoil effects in multiphoton electron-positron pair creation, *Phys. Rev. A* **82**, 013420 (2010).

- [20] A. Wöllert, H. Bauke and C. H. Keitel, Spin polarized electron-positron pair production via elliptical polarized laser fields, *Phys. Rev. D* **91**, 125026 (2015).
- [21] C. Kohlfürst and R. Alkofer, Ponderomotive effects in multiphoton pair production, *Phys. Rev. D* **97**, 036026 (2018).
- [22] Q. Z. Lv, S. Dong, Y. T. Li *et al.*, Role of the spatial inhomogeneity on the laser-induced vacuum decay, *Phys. Rev. A* **97**, 022515 (2018).
- [23] C. Kohlfürst, Effect of time-dependent inhomogeneous magnetic fields on the particle momentum spectrum in electron-positron pair production, *Phys. Rev. D* **101**, 096003 (2020).
- [24] Q. Chen, J. Y. Xiao and P. F. Fan, Gauge invariant canonical symplectic algorithms for real-time lattice strong-field quantum electrodynamics, *J. High Energ. Phys.* **2021**, 127 (2021).
- [25] L. N. Hu, O. Amat, L. Wang *et al.*, Momentum spirals in multiphoton pair production revisited, *Phys. Rev. D* **107**, 116010 (2023).
- [26] M. Jiang, R. Grobe and Q. Su, Impact of spatially periodic inhomogeneities on the photon-induced pair creation, *Phys. Rev. A* **108**, 022813 (2023).
- [27] P. Krekora, Q. Su and R. Grobe, Klein Paradox in Spatial and Temporal Resolution, *Phys. Rev. Lett.* **92**, 040406 (2004).
- [28] T. Cheng, Q. Su and R. Grobe, Introductory review on quantum field theory with space–time resolution, *Cont. Phys.* **51**, 315 (2010).
- [29] C. K. Li, D. D. Su, Y. J. Li *et al.*, Probing the spatial structure of the Dirac vacuum via phase-controlled colliding laser pulses, *Europhysics Letters* **141**, 55001 (2023).
- [30] C. C. Gerry, Q. Su and R. Grobe, *Phys. Rev. A* **74**, 044103 (2006).
- [31] G. R. Mocken, M. Ruf, C. Müller and C. H. Keitel, Nonperturbative multiphoton electron-positron–pair creation in laser fields, *Phys. Rev. A* **81**, 022122 (2010).
- [32] B. S. Xie, Z. L. Li and S. Tang, Electron-positron pair production in ultrastrong laser fields, *Matter and Radiation at Extremes* **2**, 225 (2017).